Feasibility assessment of carbon sequestration in the Grand Banks, offshore Newfoundland, Canada

Justiina T. S. Devries[1], Alexander L. Peace[1], Adedapo N. Awolayo[1,2]

[1] School of Earth, Environment, and Society, McMaster University, Hamilton, Ontario, Canada; [2] Department of Civil Engineering, McMaster University, Hamilton, Ontario, Canada

This presentation participates in OSPP — Outstanding Student & PhD candidate Presentation contest

Sharing is encouraged

Abstract EGU26-770

1 Introduction

- The Grand Banks is a structurally complex segment of the North Atlantic rift system, characterized by extensional faults, halokinesis, and heterogeneous rift basins.
- Despite advantageous geological formations, proximity to major CO_2 sources, and existing offshore infrastructure, the Grand Banks remains underexplored for Carbon Capture and Storage (CCS).
- Uncertainties in structural framework, fault architecture, and seismic history limit geological modelling needed for storage assessment.

Research Question

Are there potential sites for secure CCS integration within offshore Grand Banks, Newfoundland based on its geological and structural framework?

Objectives

- Investigate structural relationships between fault networks, salt structures, and stratigraphic sequences
- Characterize the tectono-structural evolution of the Grand Banks
- Construct and interpret the regional structural framework and basin architecture
- Identify candidate CCS sites, optimal injection locations, and safe injection thresholds to minimize induced seismicity risk

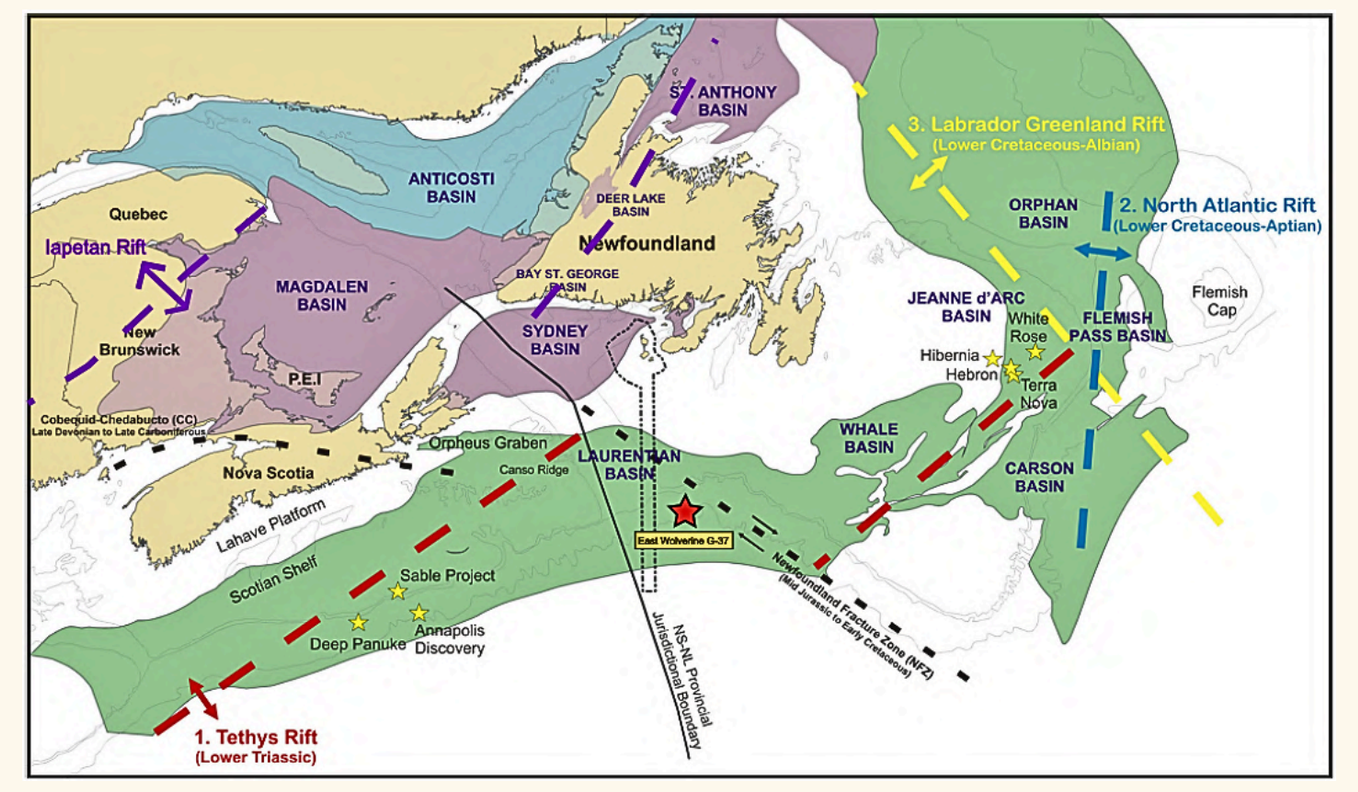


Figure 1. Tectonic elements of Canadian Atlantic Margin adapted from C-NLOPB (2012)[1].

2 Study Region and Geological Background

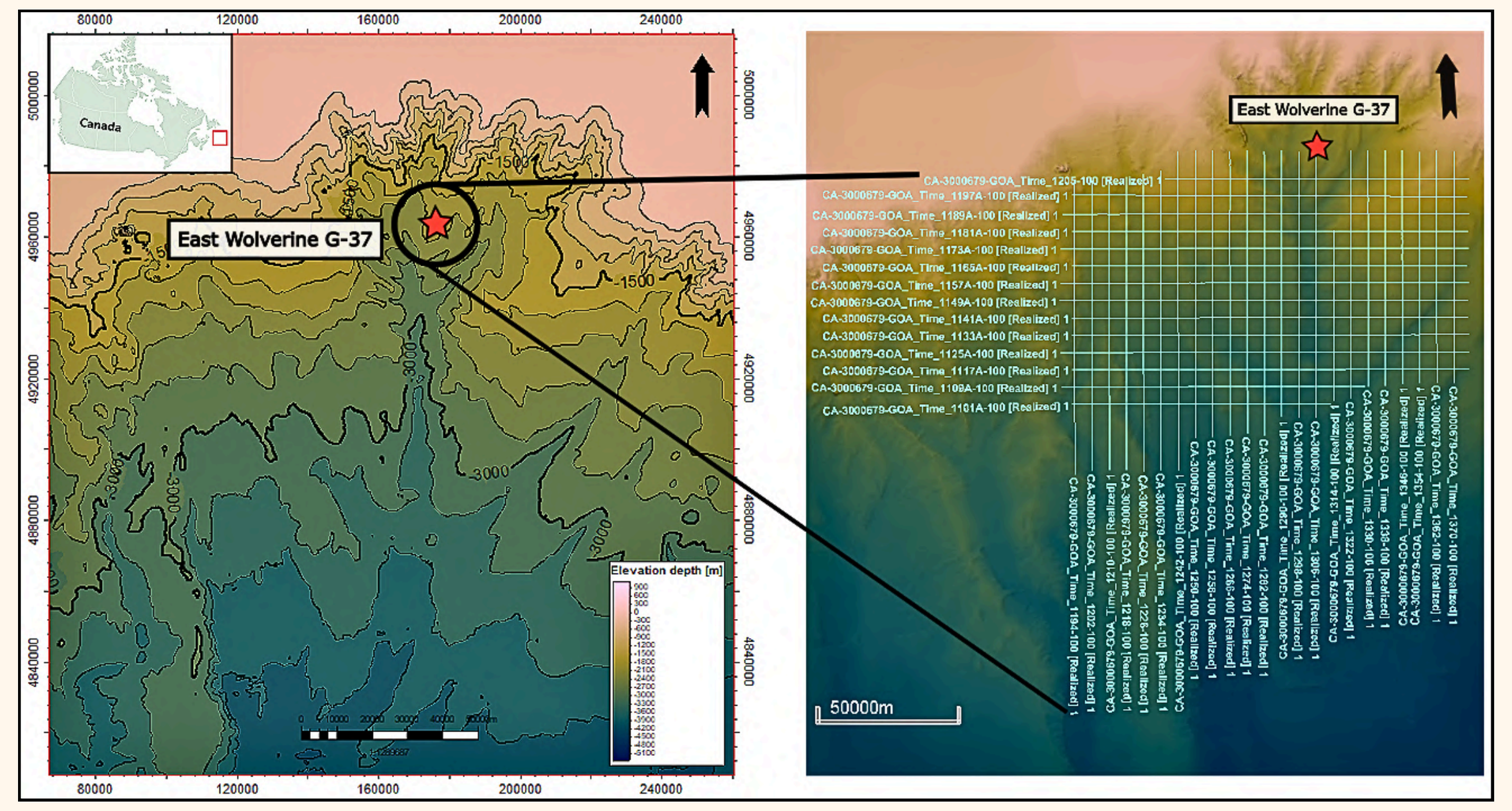


Figure 2. Bathymetry map of Grand Banks region. Red star marks the East Wolverine G-37 well location.

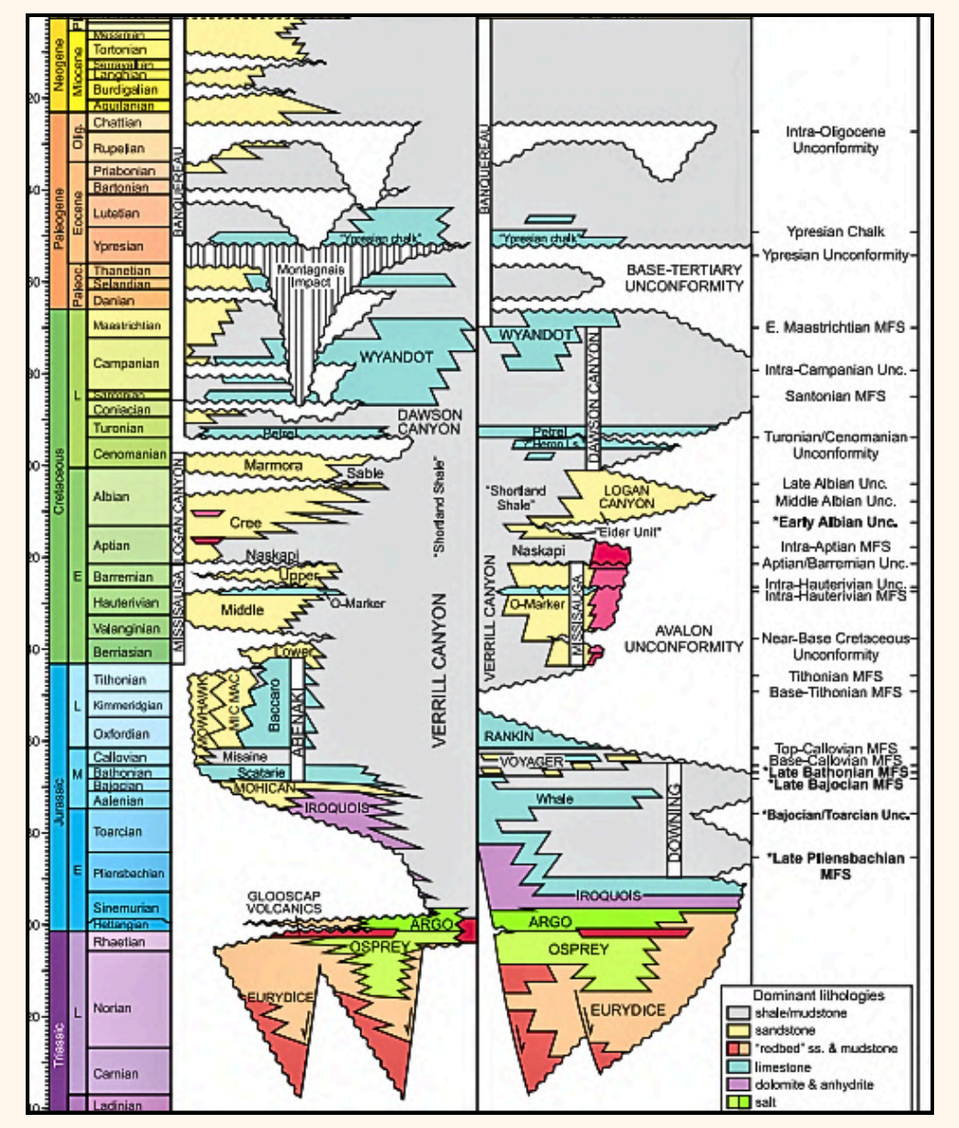
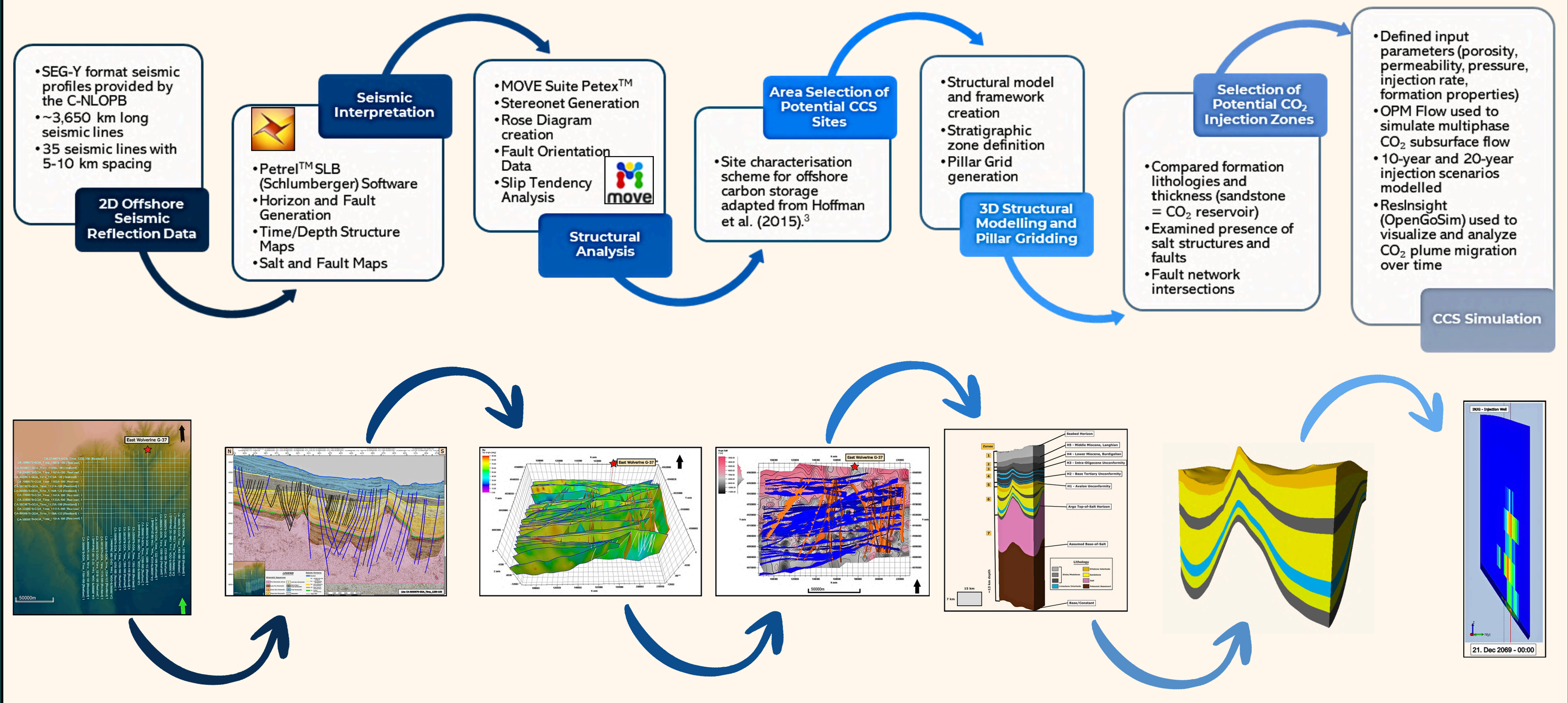


Figure 3. Mesozoic lithostratigraphy of Laurentian Basin in southern Grand Banks adapted from Weston et al. (2023)[2].

3 Methodology



Author Contact Information: devrij8@mcmaster.ca LinkedIn https://www.linkedin.com/in/justiinadevries

4 Results

A 2D Seismic Interpretation

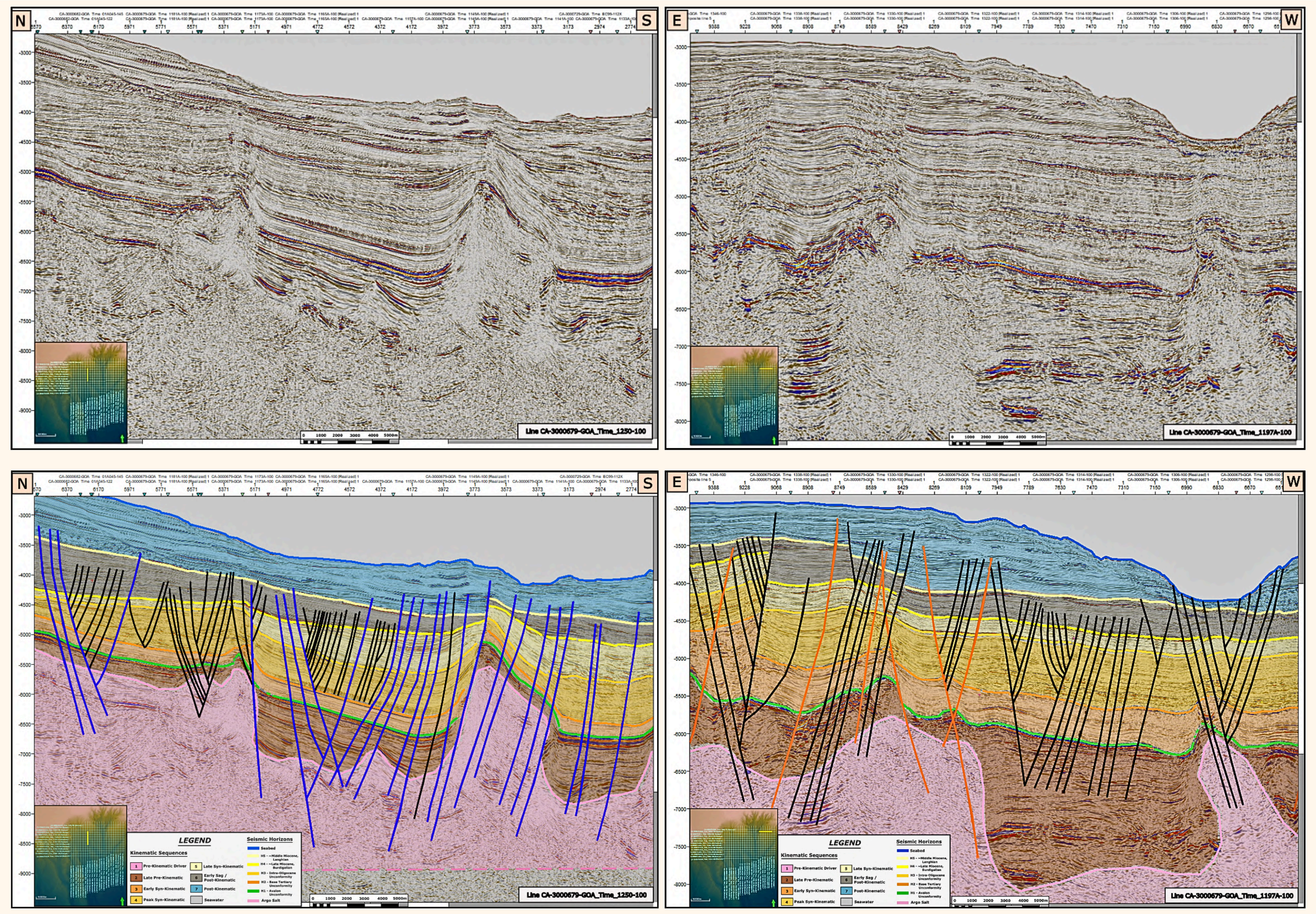


Figure 4. Uninterpreted (top) and interpreted (bottom) N-S and E-W oriented seismic profiles. Coloured fault sticks (Blue and Orange) correspond to fault interpretations incorporated into fault maps presented in Figures 7 and 8.

B Salt Tectonics and Basin Architecture

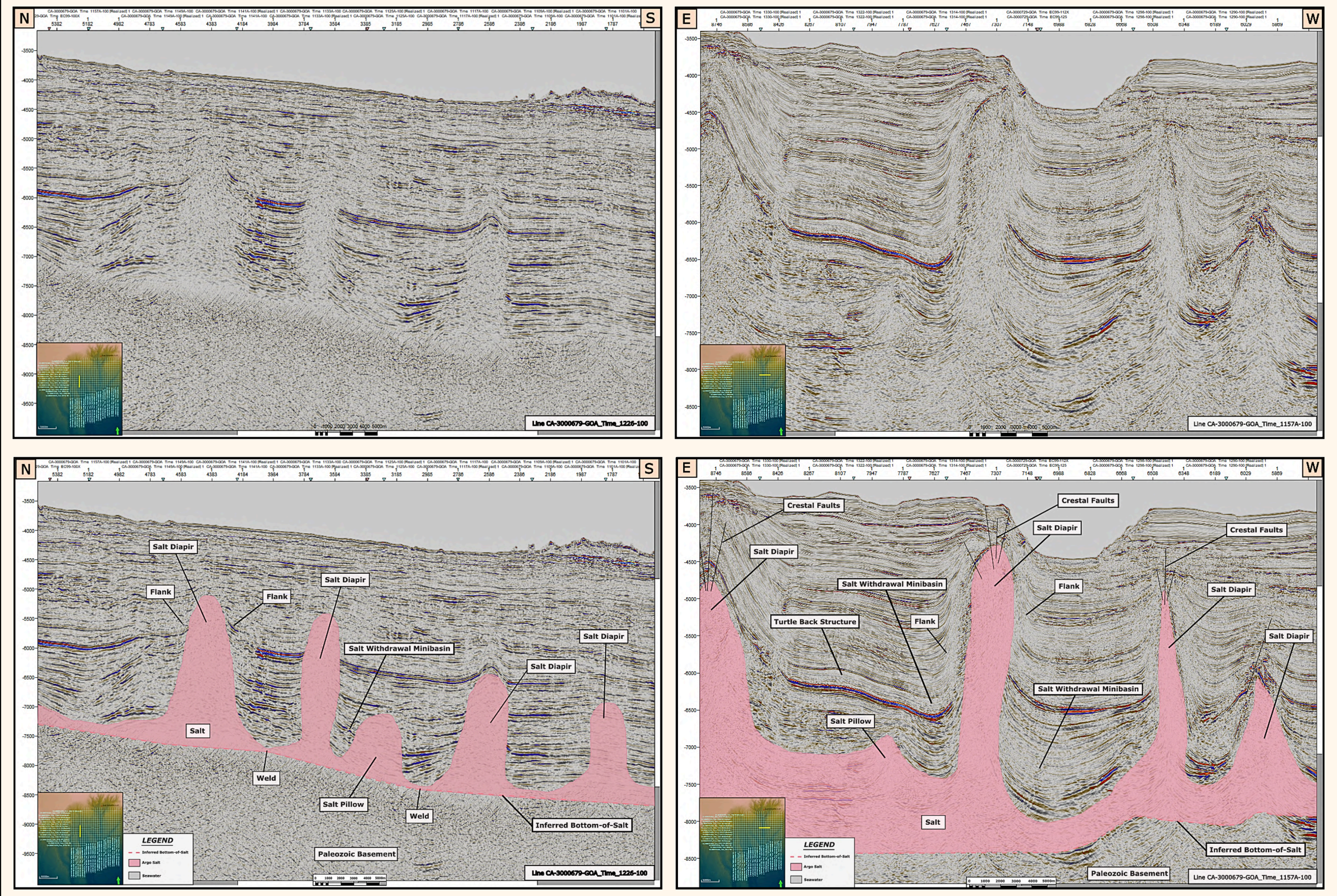


Figure 5. Uninterpreted (top) and interpreted (bottom) N-S and E-W oriented seismic profiles. Interpreted figures include annotations of salt structures (pink) present in the region.

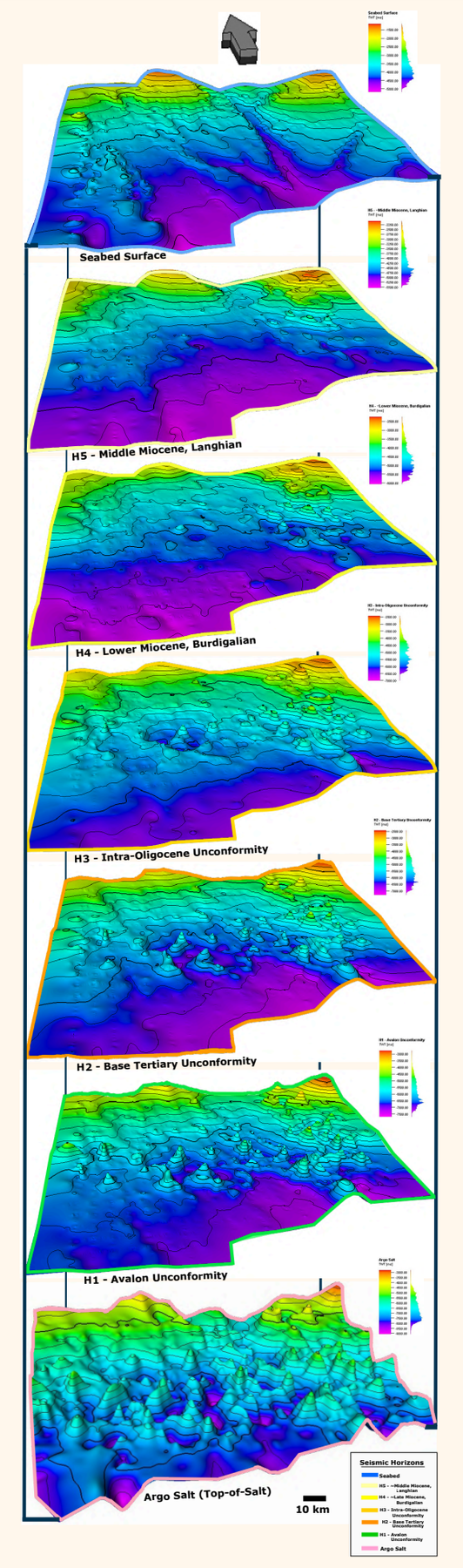


Figure 6. Time structure maps of interpreted seismic horizons.

C Fault Geometry and Structural Framework Analysis

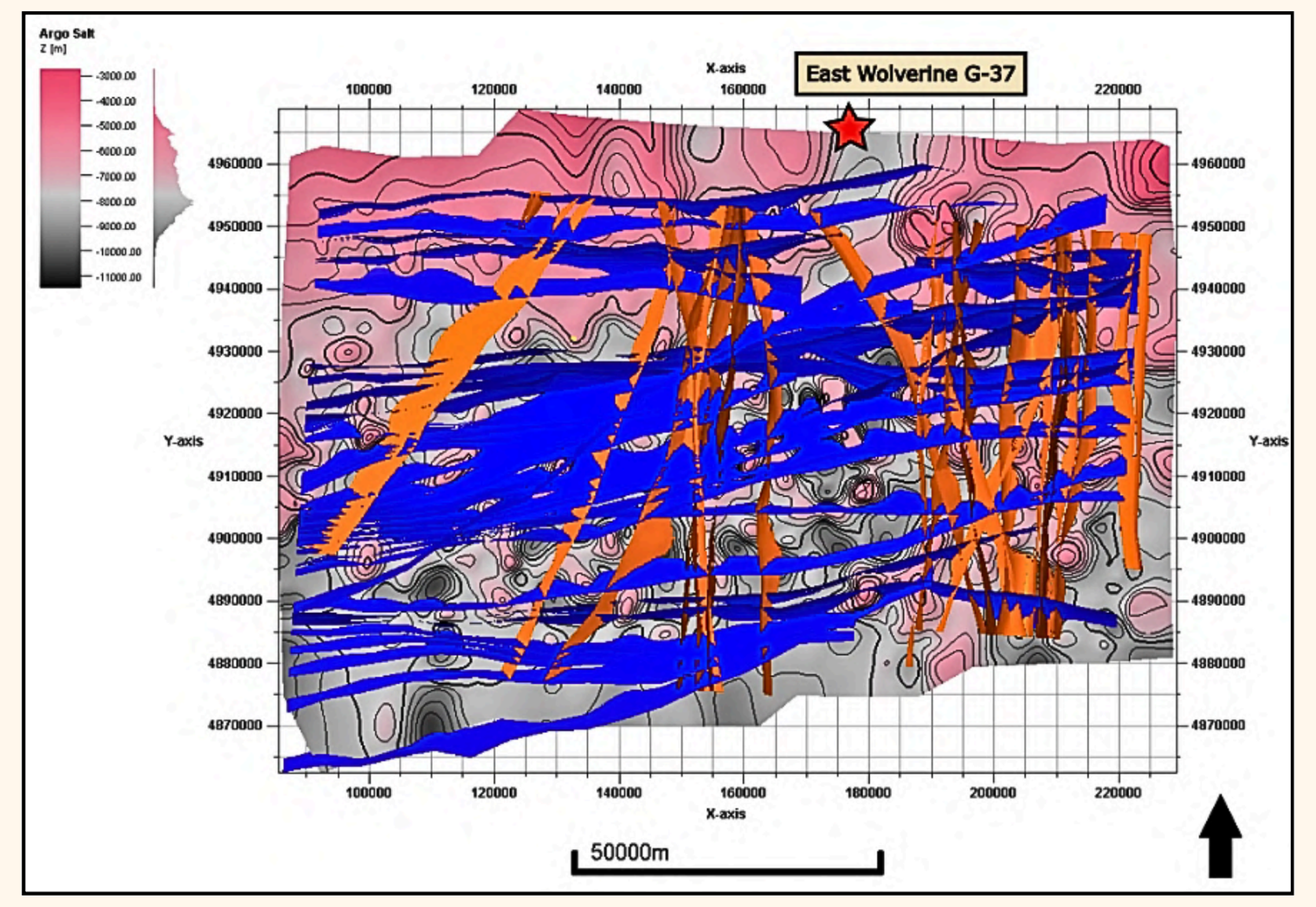


Figure 7. 2D fault map overlayed with Top-of-Salt depth structure map (Argo Formation). Two fault populations trending ~N-S (orange) and E-W (blue). The East Wolverine G-37 well is marked with red star.

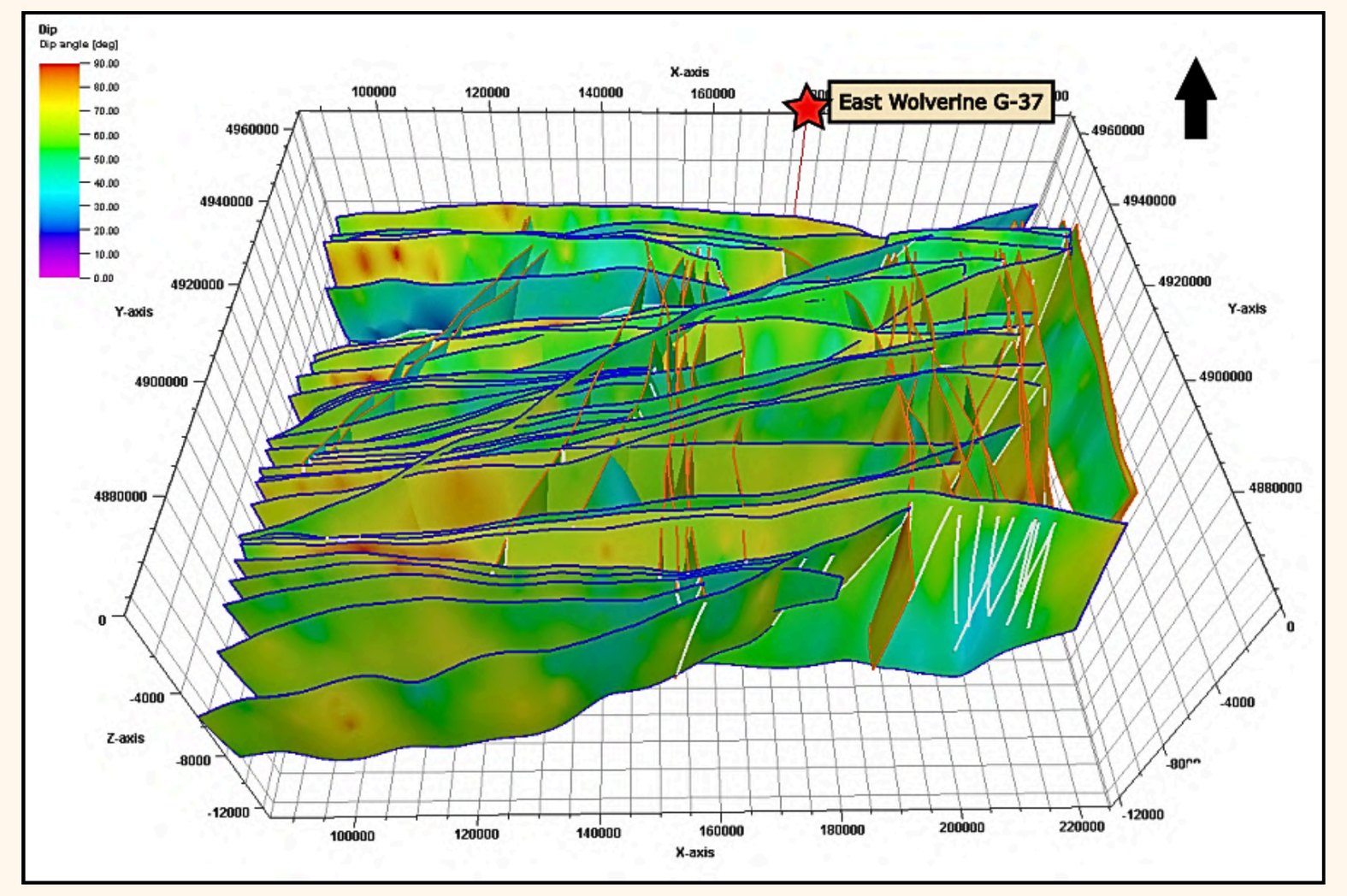


Figure 8. 3D fault map with Dip Angle attribute (degrees). The East Wolverine G-37 well is marked with red star.

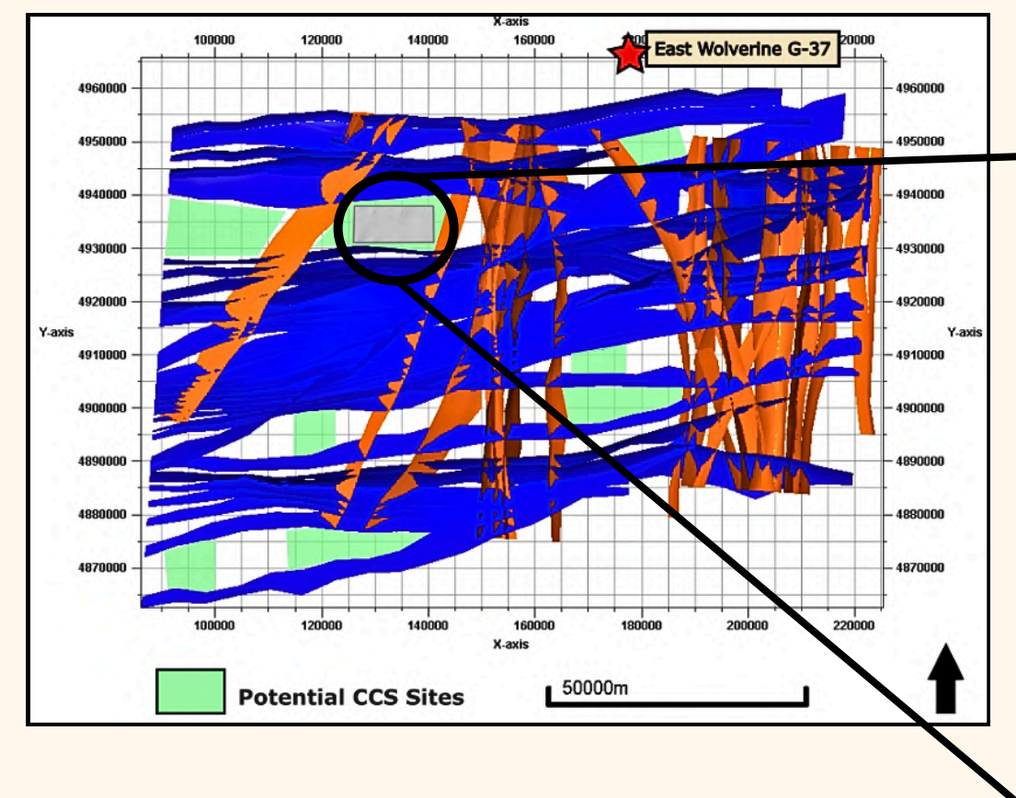


Figure 9. 2D fault map depicting 2 fault populations (blue and orange) marked with potential sites for CCS integration. The East Wolverine G-37 well is marked with red star.

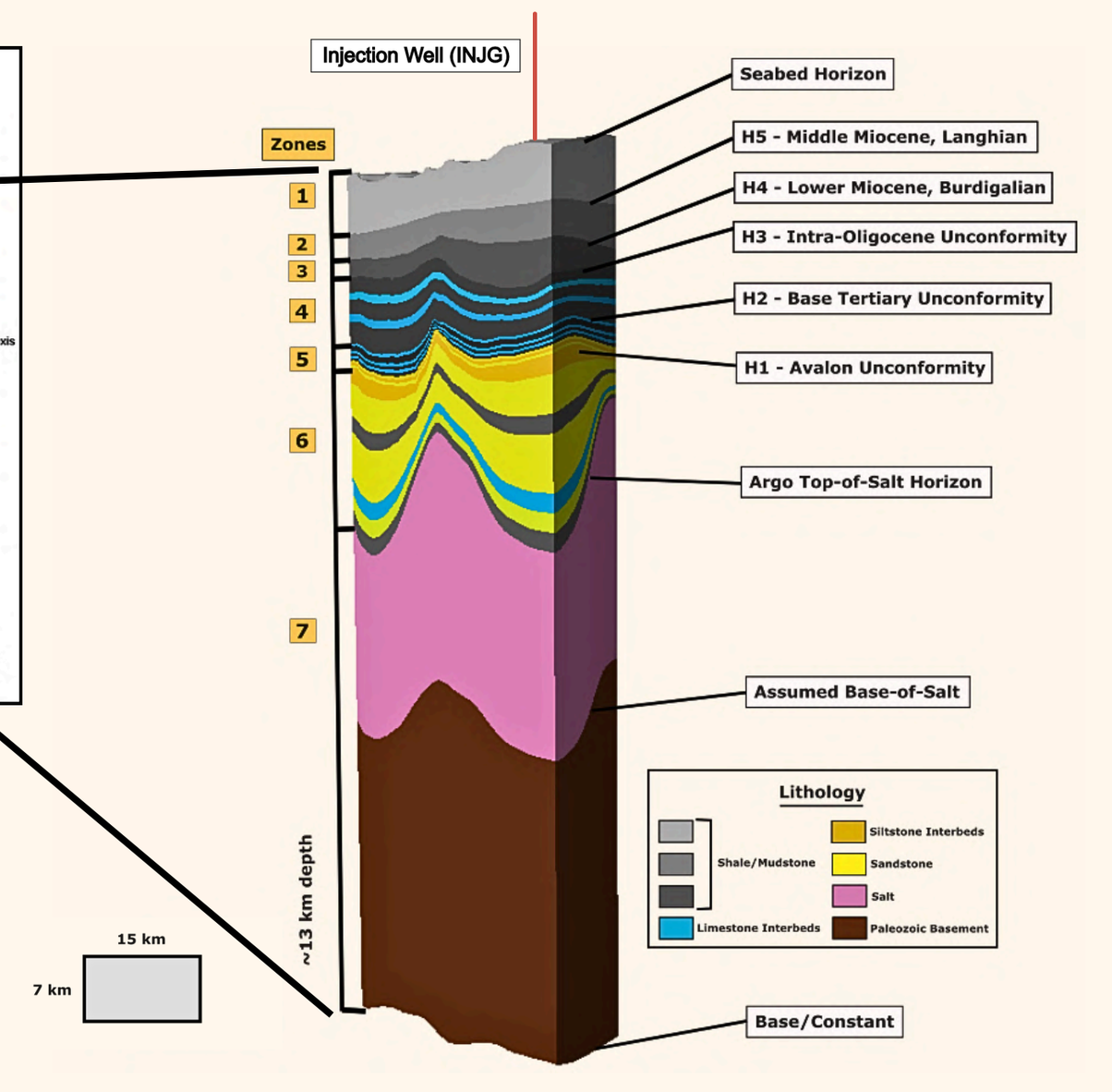


Figure 10. 3D pillar grid of a 15 km x 7 km region that was identified as a potential CCS site.

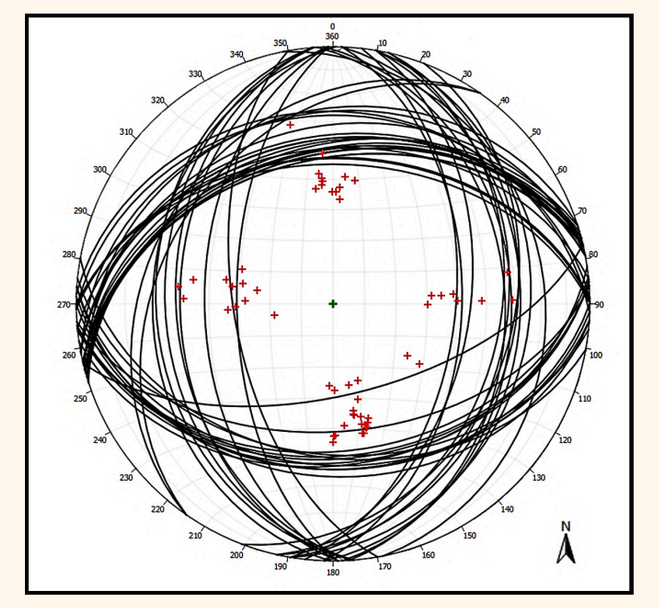


Figure 11. Stereonet plot depicting two fault populations based on fault strike orientations.

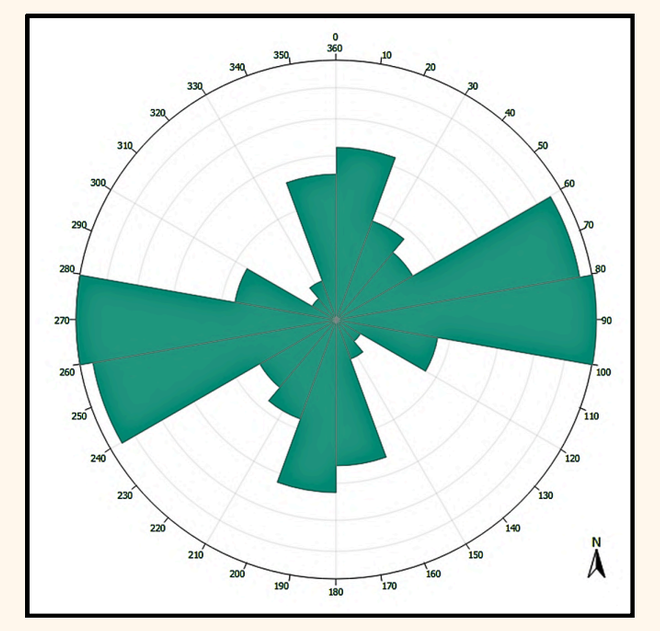


Figure 12. Bidirectional rose diagram of fault strike orientations showing two fault populations trending ~ N-S and E-W.

- Fault maps reveal two distinct N-S and E-W normal fault sets associated with widespread salt structures, graben, and half-graben structures, indicating Mesozoic extension and coupled fault-salt evolution.
- This presents a complex yet strategically favourable setting where faults may act as barriers or conduits for fluid flow, while salt influences trapping efficiency.

D Slip Tendency Stress Orientation Scenarios

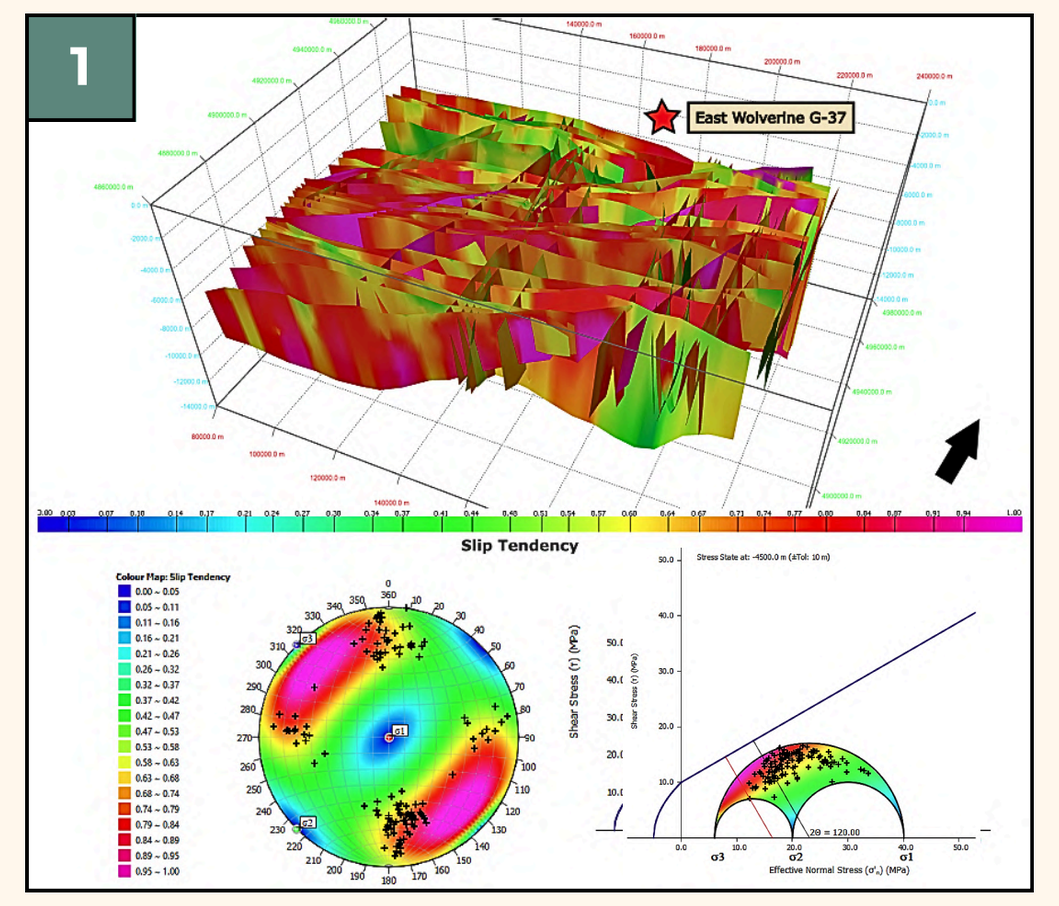


Figure 13. Slip tendency fault map Scenario 1: Present-day stress orientation estimate constrained from World Stress Map by Heidbach et al. (2025)[4].

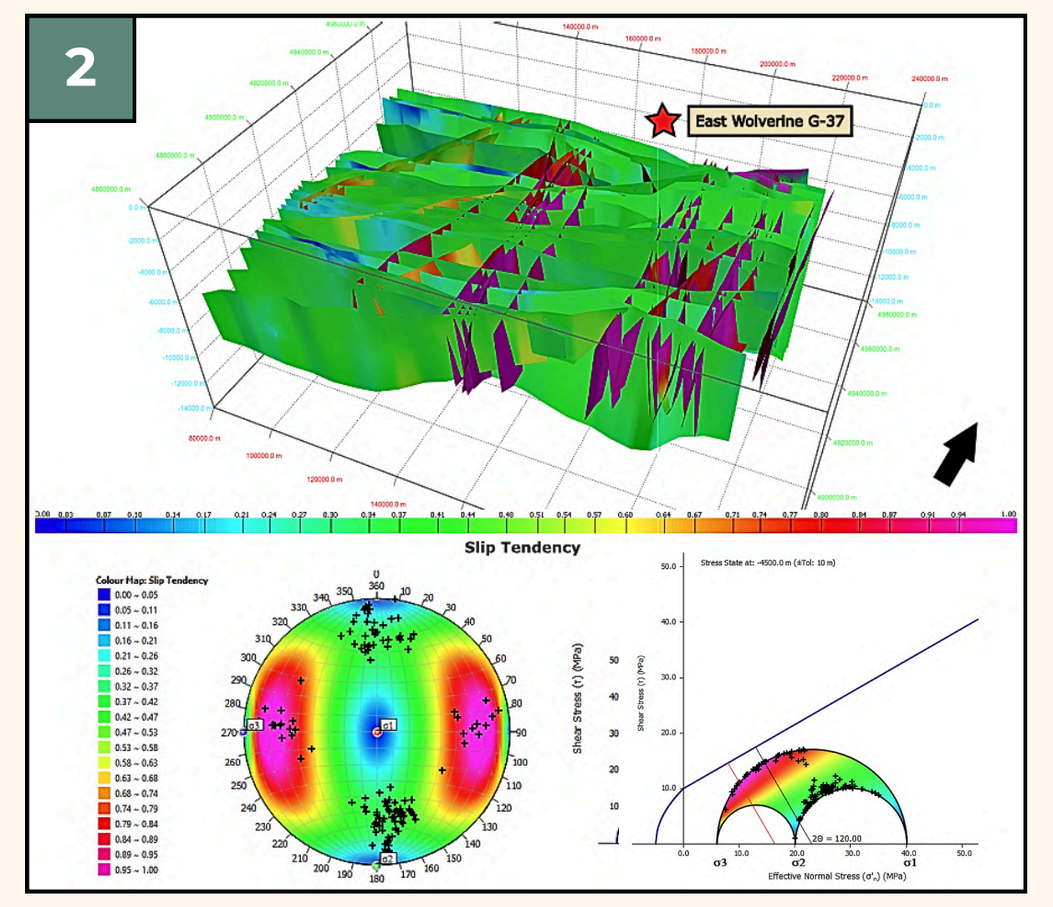


Figure 14. Slip tendency fault map Scenario 2: Strike-parallel extension, minimum reactivation end-member.

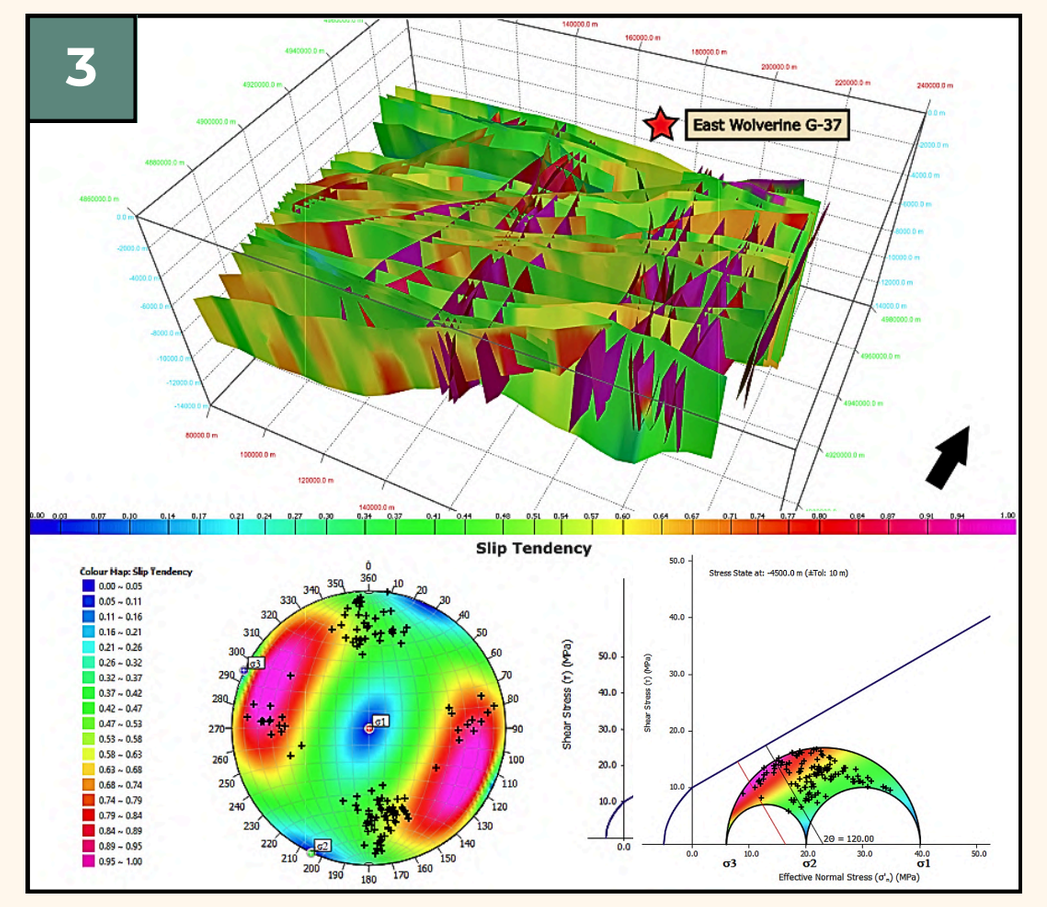


Figure 15. Slip tendency fault map Scenario 3: Optimally-oriented failure, maximum reactivation end-member.

σ_1 is vertical (plunge = 90°) at 4,500 m for all scenarios. Only horizontal stress azimuths vary between scenarios.

Slip Tendency Stress Orientations (Plunge/Azimuth)	σ1	σ2	σ3	Fracture Stability
Scenario 1	90/135	0/045	0/135	5.0 MPa
Scenario 2	90/135	0/000	0/090	5.2 MPa
Scenario 3	90/045	0/025	0/115	3.2 MPa

- N-S faults maintain high slip tendency (Ts > 0.75) across all scenarios, indicating reactivation potential independent of stress field orientation uncertainty.
- E-W faults are stress-sensitive, with low Ts when σ3 is fault-parallel (Scenario 2) and moderate-high Ts as σ3 rotates to 115°-135° (Scenarios 1 and 3).
- Contrasting Ts behaviour of fault populations suggests a structurally complex margin origin involving both orthogonal extension and strike-slip deformation, consistent with a transform component in the margin's structural inheritance.
- Local stress regime remains poorly constrained due to limited WSM 2025[4] coverage in region (stress indicators provided for Scotian Margin, coverage does not extend into hinge zone between Cobequid-Chedabucto Fault System and Newfoundland Fracture Zone).

E CO_2 Injection Simulations

1 10-Year Injection Simulation

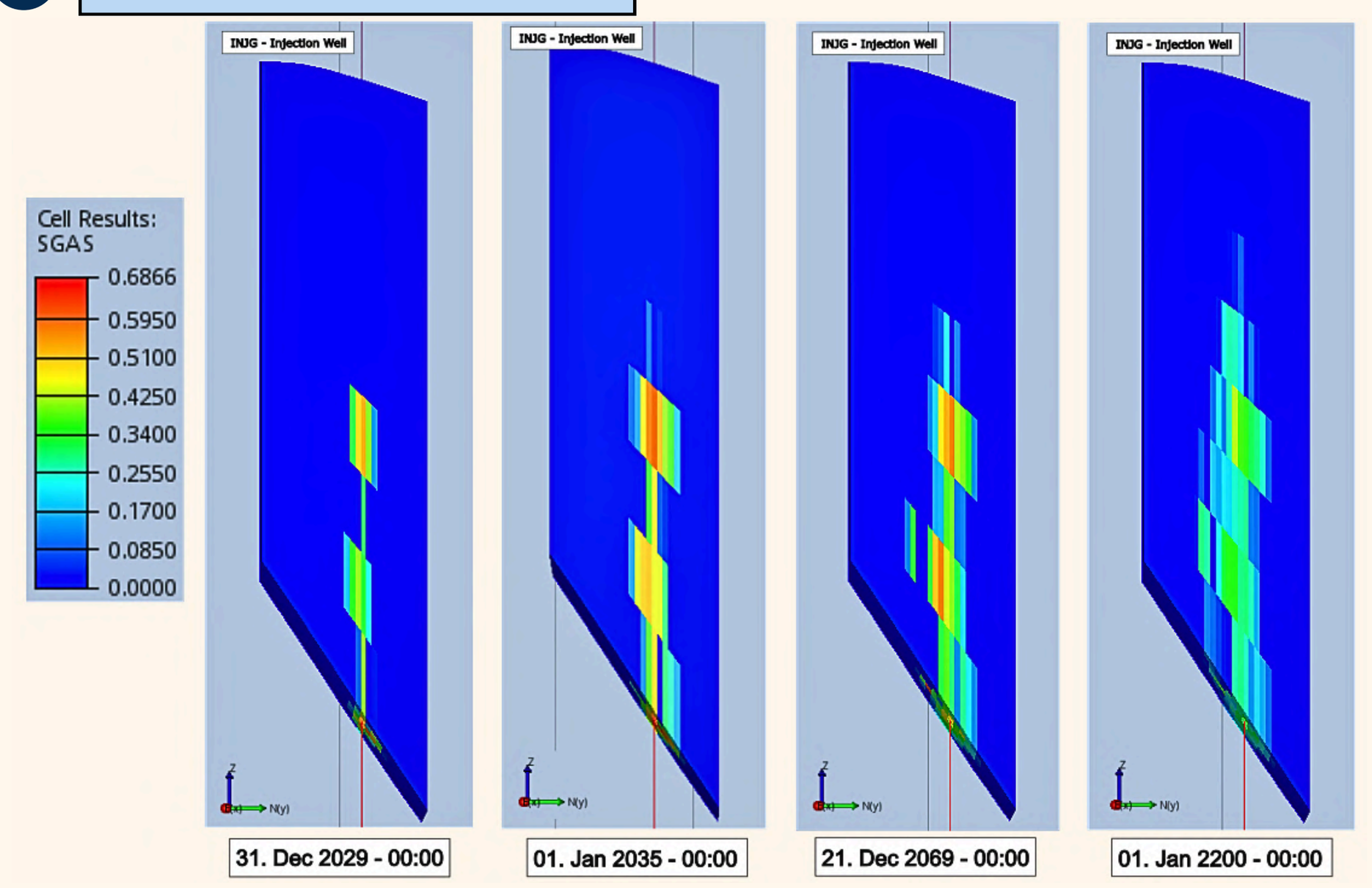


Figure 16. 10-year CO_2 injection simulation in target Zone 6 (Figure 15) at a depth of 4578 m below seabed. 1 Mt/year was injected over 10 years (10 Mt total), with plume migration monitored over a 175-year simulation period (Jan 2025 - Jan 2200).

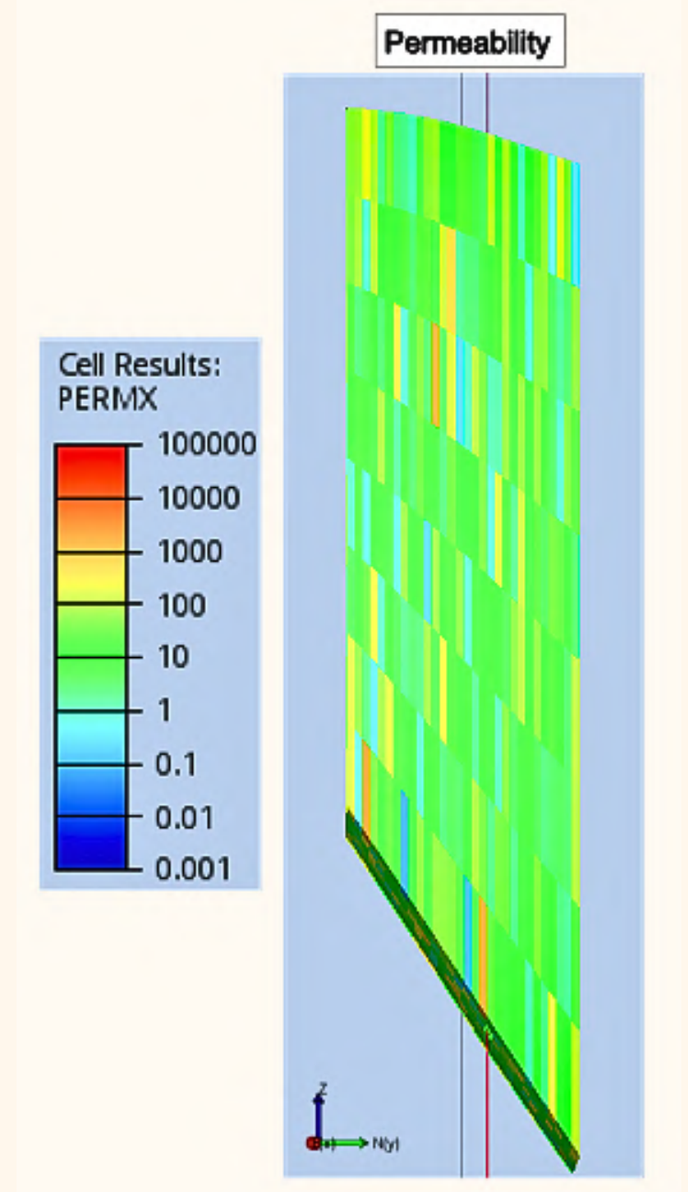


Figure 17. 3D permeability model (PERMX) of target Zone 6 in Simulation 1.

2 20-Year Injection Simulation

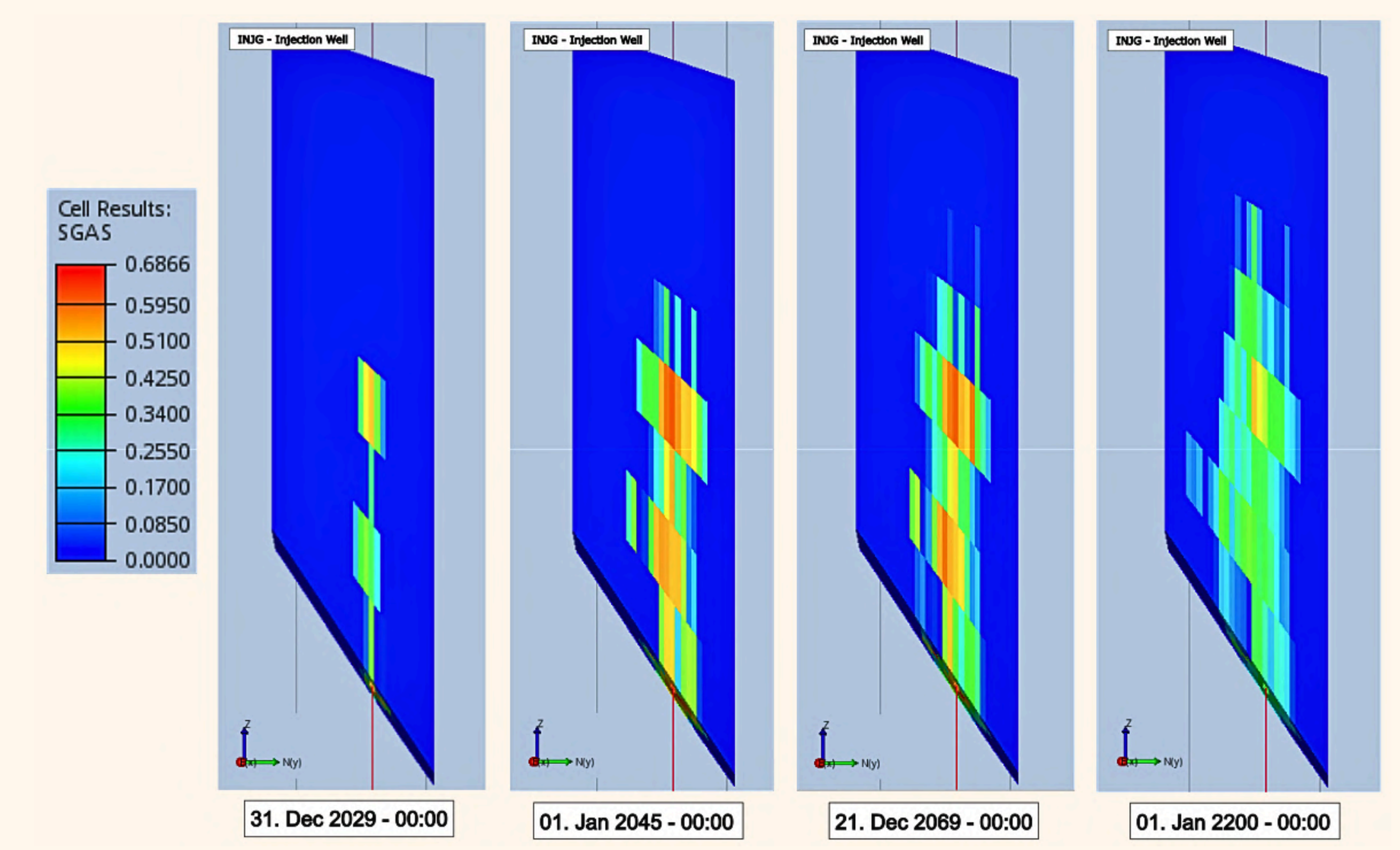


Figure 18. 20-year CO_2 injection simulation in target Zone 6 (Figure 15) at a depth of 4578 m below seabed. 1 Mt/year was injected over 20 years (20 Mt total), with plume migration monitored over a 175-year simulation period (Jan 2025 - Jan 2200).

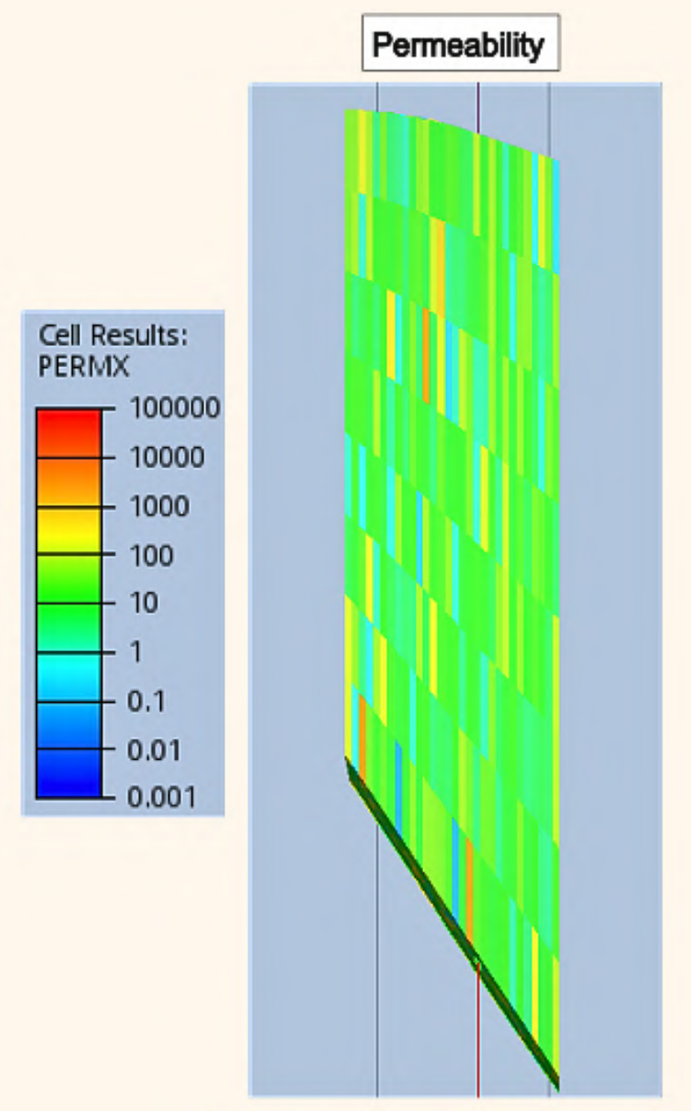


Figure 19. 3D permeability model (PERMX) of target Zone 6 in Simulation 2.

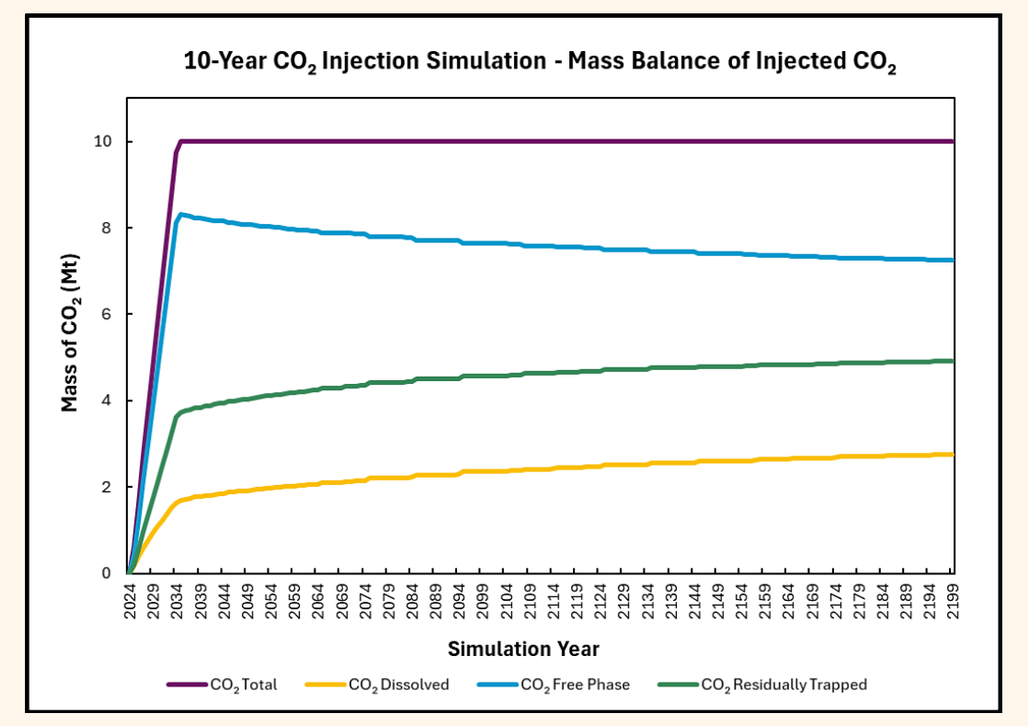


Figure 20. Mass balance of injected CO_2 for the 10-year injection simulation (10 Mt total). Free phase CO_2 decreases after injection ceases in 2035, while residual and dissolution trapping increase over 175 years.

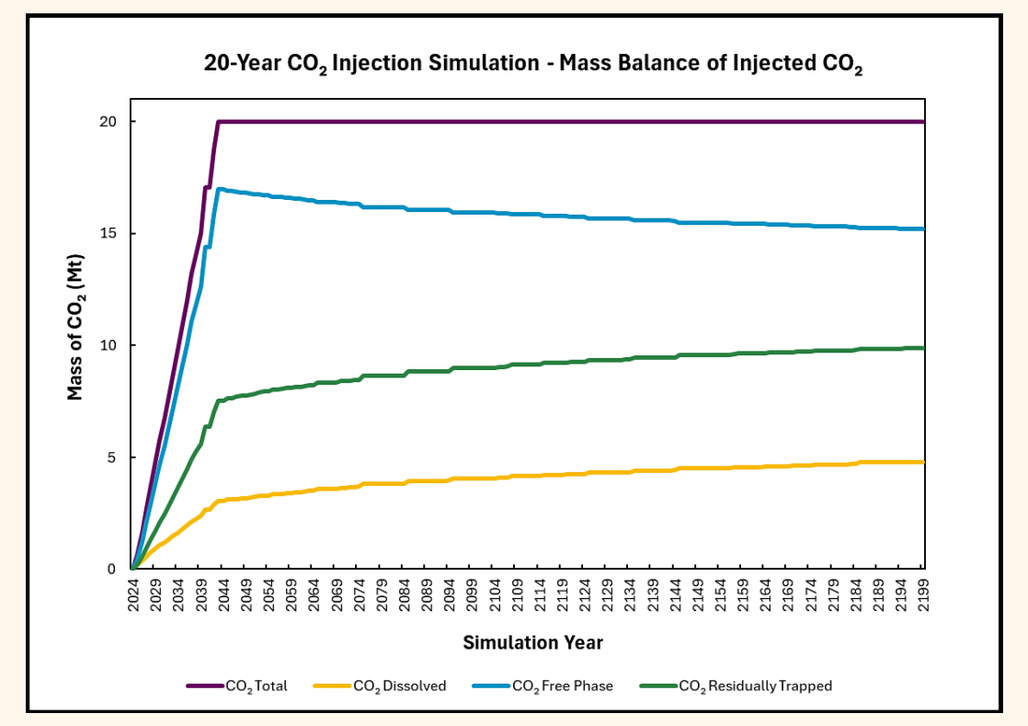


Figure 21. Mass balance of injected CO_2 for the 20-year injection simulation (20 Mt total). Despite double the injected volume, residual and dissolution trapping continue to increase throughout post-injection monitoring period.

5 Key Takeaways

1. N-S and E-W fault trends and salt-fault interactions reveal a heterogeneous margin shaped by multiple phases of rifting, strike-slip deformation, and structural inheritance which is inconsistent with a simple passive margin model.
2. The hinge zone between the Cobequid-Chedabucto Fault System and the Newfoundland Fracture Zone may record a transform-rift transition where earlier strike-slip deformation was overprinted by later extension; however, this requires further investigation.
3. Both simulations show CO_2 migration toward salt diapir flank with the 20-year scenario producing a larger plume (20 Mt vs 10 Mt). Both demonstrate effective containment and trapping within Zone 6. Future work incorporating faults and salt geometry is needed to fully assess storage security.

6 Acknowledgements and References

This work was supported by NSERC Discovery Grant funding and associated research programs. Thank you to the McMaster Structural Geology and Tectonics Research group for their continued support, and to our collaborators in the McMaster Department of Civil Engineering for their valuable contributions. We would also like to thank the Canada-Newfoundland and Labrador Offshore Petroleum Board (C-NLOPB) for the seismic data, SLB (Schlumberger) for Petrel, PE Ltd. for MOVE, OpenGoSim for ResInsight, and Open Porous Media Initiative for OPM Flow. Lastly, thank you to the Canadian Energy Geosciences Association (CEGA) for granting the Regional Graduate Scholarship for this work.

References